Computations and Aeroelastic Applications of Unsteady Transonic Aerodynamics About Wings

P. Guruswamy*
Informatics General Corporation, Palo Alto, California
and
P. M. Goorjian*
NASA Ames Research Center, Moffett Field, California

Comparisons were made of computed and experimental data in three-dimensional unsteady transonic aerodynamics, including aeroelastic applications. The computer code LTRAN3, which is based on small-disturbance aerodynamic theory, was used to obtain the aerodynamic data. A procedure based on the *U-g* method was developed to compute flutter boundaries by using the unsteady aerodynamic coefficients obtained from LTRAN3. The experimental data were obtained from available NASA publications. All of the studies were conducted for thin, unswept, rectangular wings with circular-arc cross sections. Numerical and experimental steady and unsteady aerodynamic data were compared for a wing with an aspect ratio of 3 and a thickness ratio of 5% at Mach numbers of 0.7 and 0.9. Flutter data were compared for a wing with an aspect ratio of 5. Two thickness ratios, 6% at Mach numbers of 0.715, 0.851, and 0.913, and 4% at Mach number of 0.904, were considered. Based on the unsteady aerodynamic data obtained from LTRAN3, flutter boundaries were computed; they were compared with those obtained from experiments and the code NASTRAN, which uses linear aerodynamics.

Nomenclature

a_h = distance between midchord and elastic axis measured in semichords, positive toward the trailing edge
b = semichord length
c = full-chord length
$C_{l\alpha}$ = sectional lift coefficients due to h and α modes, respectively
$C_{m\alpha}$ = sectional moment coefficients due to h and α modes, respectively
C_p = pressure coefficient
g_h = structural damping corresponding to h mode
g_α = structural damping corresponding to α mode
h = bending displacement of elastic axis
I_α = sectional polar moment of inertia about elastic axis
k_b = reduced frequency defined as wb/U
k_c = reduced frequency defined as $\omega c/U$
l = semispan length of the wing
m = mass of the wing per unit span
r_α = $(I_\alpha/mb^2)^{1/2}$, radius of gyration about elastic axis
S_α = sectional static moment about elastic axis
U = freestream velocity
x_α = S_α/mb, distance in semichords measured from elastic axis to mass center of the wing section
α = rotation of the wing section about the elastic axis
γ = ratio of specific heats
Δ = unsteady pressure jump
λ = flutter eigenvalue
μ = $m/\pi\rho b^2$, wing-to-air-mass density ratio
ξ = h/b, nondimensional bending displacement
ρ = freestream density
τ = ratio of maximum thickness of wing cross section to chord length
ϕ = disturbance velocity potential
ω_h = uncoupled natural frequency of h mode
ω_α = uncoupled natural frequency of α mode

Presented at the AIAA/ASME/ASCE/AHS 23rd Structures, Structural Dynamics, and Materials Conference, New Orleans, La., May 10-12, 1982; submitted May 12, 1982; revision received June 23, 1983. This paper is declared a work of the U.S. Government and therefore is in the public domain.

*Research Scientist. Member AIAA.

Introduction

EXTENSIVE experimental and numerical studies have been conducted recently in the area of transonic aerodynamics and aeroelasticity. Such studies are important because the transonic regime plays an important role in the design of modern aircraft. A review of the state-of-the-art of transonic flow computations was given by Ballhaus et al.,[1] and developments in experimental and theoretical transonic aerodynamics for aeroelastic applications were reviewed by Ashley.[2]

Both experimental and theoretical studies are quite complicated in the transonic regime, because the equations governing the flow are nonlinear, and these flows are characterized by the presence of shock waves. Studies have shown that for the case of flows at Mach numbers near 1, small-amplitude motions can cause large variations in the aerodynamic forces and moments. Because of these special characteristics of transonic flows, the probability of encountering aeroelastic instabilities is higher. For example, it has been found both experimentally and theoretically that flutter boundary curves show a dip in the transonic range.[3]

During the last decade various computer codes have been developed to compute unsteady transonic aerodynamics for aeroelastic applications. In particular, codes that solve the small-disturbance potential equations for transonic flows about oscillating airfoils, such as LTRAN2,3 are now used routinely.[4,5] Similar codes are now being developed for the computation of three-dimensional unsteady aerodynamics.

In Ref. 6, Traci et al. reported the development of the three-dimensional steady and unsteady small-disturbance codes, TDSTRN and TDUTRN, respectively. The unsteady code TDUTRN is based on the harmonic method where an unsteady solution is linearized with respect to time. Thus, it is limited to cases with small oscillations. Eastep and Olsen[7] applied these codes for the computation of flutter boundaries of a rectangular wing by using the *U-g* method.

As an alternative, but more complete method, Borland et al.[8] have developed a three-dimensional, unsteady, small-disturbance transonic low-frequency code, LTRAN3 based on a time-integration method. In this code, the finite difference scheme developed for two-dimensional flows[3] was extended to three-dimensional flows over wings. A demonstration calculation of the code was performed by computing the unsteady loads on a swept wing with an NACA 64A010 airfoil section at Mach number 0.9. In Ref. 9, Borland and Rizzetta developed a modified code, XTRAN3S. In this code high-frequency effects are incorporated in both the governing differential equation and the boundary conditions. It also has the capability of performing static and dynamic aeroelastic computations by simultaneously integrating the aerodynamic and structural equations of motion. Borland and Rizzetta illustrated this capability by computing flutter boundaries for a rectangular wing with a 6% thick parabolic-arc airfoil section at Mach numbers of 0.8, 0.85 and 0.875. These codes, which are candidates for use in research and industrial applications, have yet to be compared with experimental results.

Parallel to these theoretical attempts, several experimental studies were conducted in the areas of transonic aerodynamics and aeroelasticity.[10-14] These experiments can be used independently to help in understanding physical phenomena and to provide an experimental data base for the assessment of new computer codes. Because of the complexity of transonic aerodynamics, it is necessary to compare experimental and theoretical results in detail.

In this study, aerodynamic and aeroelastic results obtained by the unsteady, small-disturbance transonic code LTRAN3 are compared with the corresponding experimental results available from NASA.[11-13] Unswept, rectangular, flexible wings with thin circular-arc airfoil sections are considered for flows in the transonic Mach number range.

In order to compare aerodynamic results from LTRAN3 and experiment, a case of a rectangular wing that was experimentally studied in Ref. 11 was selected at Mach numbers of 0.7 and 0.9. The wing has circular-arc airfoil sections of maximum thickness-to-chord ratio of 5%, and was subjected to oscillatory motion in the first bending mode. Both steady and unsteady pressure distributions obtained from LTRAN3 and experiment are compared at four span stations for Mach numbers of 0.7 and 0.9. Unsteady results are presented in the form of chordwise distributions of pressure coefficients in magnitude and phase angle. These results are also compared with corresponding results obtained by linear aerodynamic theory.

To compare flutter results obtained by using unsteady aerodynamic coefficients from LTRAN3 with experimental data,[13] four cases of a rectangular wing with circular-arc airfoil cross sections were considered. The cases considered were: 1) 6% thick at $M=0.715$, 2) 6% thick at $M=0.851$, 3) 6% thick at $M=0.913$, and 4) 4% thick at $M=0.904$.

In Ref. 9 the simultaneous integration method was employed to obtain flutter boundaries. Although this method is accurate for the transonic regime, it has some disadvantages when it has to be used alone. The method requires aeroelastic parameters that are close to flutter as an input in order to find the flutter boundary. If the aeroelastic parameters are not close to the flutter boundary, it may take several computationally expensive attempts to obtain the flutter boundary. In addition it may not give undamped motion for all of the assumed modes unless the aeroelastic parameters are exactly the same as that for the flutter boundary.

In this study an alternative procedure based on the *U-g* method is used to obtain the flutter boundary. When compared with the procedure used in Ref. 9, the present procedure requires the additional assumption that the principle of superposition of airloads is valid. This principle is valid even in the presence of shocks when the amplitude of oscillations is small.[3,15] Since the flutter equations are based on small amplitudes of oscillations, the superposition principle is valid in this study. Such assumptions have led to successful methods for predicting the flutter of airfoils in the transonic regime.[16] As suggested in Ref. 16, a combination of the procedure given in Ref. 9 and the present procedure may lead to an efficient way of predicting the flutter boundaries of wings in the transonic regime for airfoils.

To obtain flutter boundaries by the *U-g* method, unsteady aerodynamic coefficients were computed from LTRAN3 for two assumed modes at three selected reduced frequencies. Flutter results are presented in the form of plots of flutter speed and corresponding reduced frequency vs wing-air density ratio. These results are compared with experiments and also with those results obtained from the computer code NASTRAN, which uses linear aerodynamics based on the doublet-lattice method.

Aerodynamic Equations of Motion

Many forms of the small-disturbance equations have been developed for computing the transonic flowfield about wings.[17,18] In this analysis the modified unsteady, three-dimensional, transonic small-disturbance equation is used.

$$A\phi_{tt}+B\phi_{xt}=(E\phi_x+F\phi_x^2+G\phi_y^2)_x + (\phi_y+H\phi_x\phi_y)_y+(\phi_z)_z \tag{1}$$

where ϕ is the disturbance velocity potential; $A=M_\infty^2$; $B=2M_\infty^2$; $E=(1-M_\infty^2)$; $F=\frac{1}{2}(\gamma+1)M_\infty^2$; $G=\frac{1}{2}(\gamma-3)M_\infty^2$; and $H=-(\gamma-1)M_\infty^2$.

The low-frequency form of this equation is solved in the computer code LTRAN3 by setting A to zero and using corresponding boundary conditions. This code is based on a time-marching, finite difference scheme following the first-order accurate alternating direction implicit (ADI) algorithm. A detailed description of the procedure can be found in Ref. 19. It is the first time that a computer code has been developed by extending the ADI algorithm from two to three dimensions. Preliminary comparisons with other theoretical methods have shown that the ADI method can be used satisfactorily to solve Eq. (1); however, it is necessary to validate the method by making detailed comparisons with experiments.

For the cases considered in this study, a Cartesian grid was used with 60 points in the streamwise direction, 40 points in the vertical direction, and 20 points in the spanwise direction. The wing surface was defined by 39 points in the streamwise direction and 13 points in the spanwise direction. Computational boundaries were located as follows: upstream boundary at 15.4 chords, downstream boundary at 26.6 chords, far-span boundary at 1.6 semispan, above the wing at 13.0 chords, and below the wing at 13.0 chords.

Steady aerodynamic pressures were computed by integrating Eq. (1) in time and setting the steady boundary conditions on the airfoil. LTRAN3 does not compute the residuals of the velocity potential to determine the convergence of the steady-state solution. Convergence is determined based on the pressures. The integration procedure is stopped when the maximum pressure on the wing does not change by more than about 0.1% over 100 time steps. The number of time steps required for convergence depends mainly on the Mach number. For the cases considered in this study, the number of time steps required was between 600 and 1000.

Unsteady aerodynamic pressures were computed by forcing the wing to undergo a sinusoidal modal motion and integrating the aerodynamic equation of motion in time. The modal motion assumed was the same as that simulated in the experiments. For all of the cases studied here it was found that about three cycles of motion with 360 time steps per cycle were sufficient to obtain a periodic aerodynamic response. Periodicity was tested by comparing the responses of the second and third cycles. The magnitudes and phase angles of

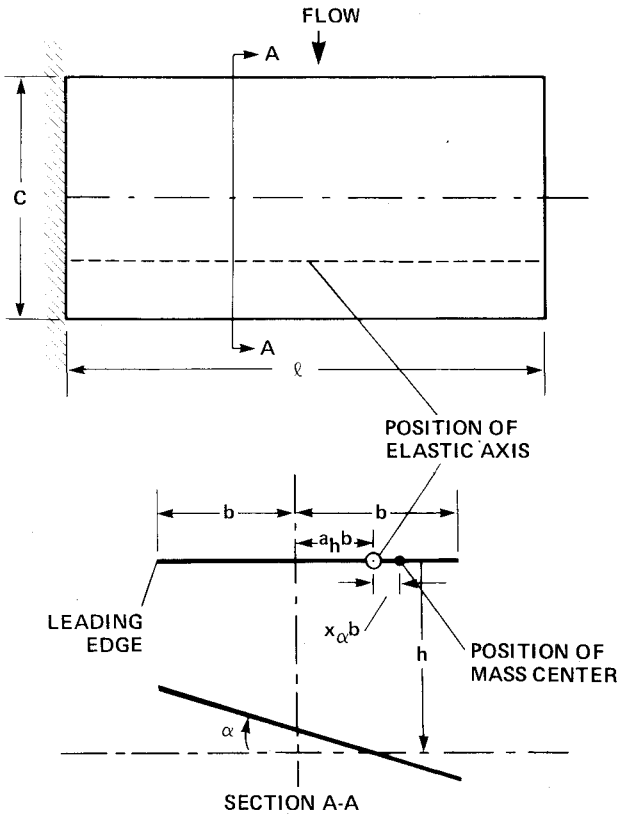

Fig. 1 Definition of aeroelastic parameters for a cantilever wing.

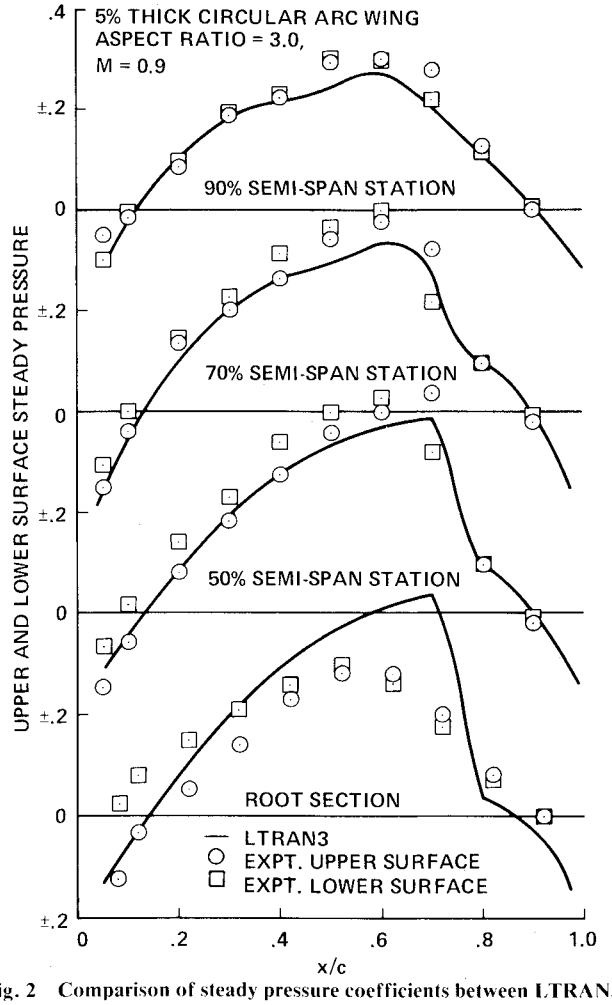

Fig. 2 Comparison of steady pressure coefficients between LTRAN3 and experiment.

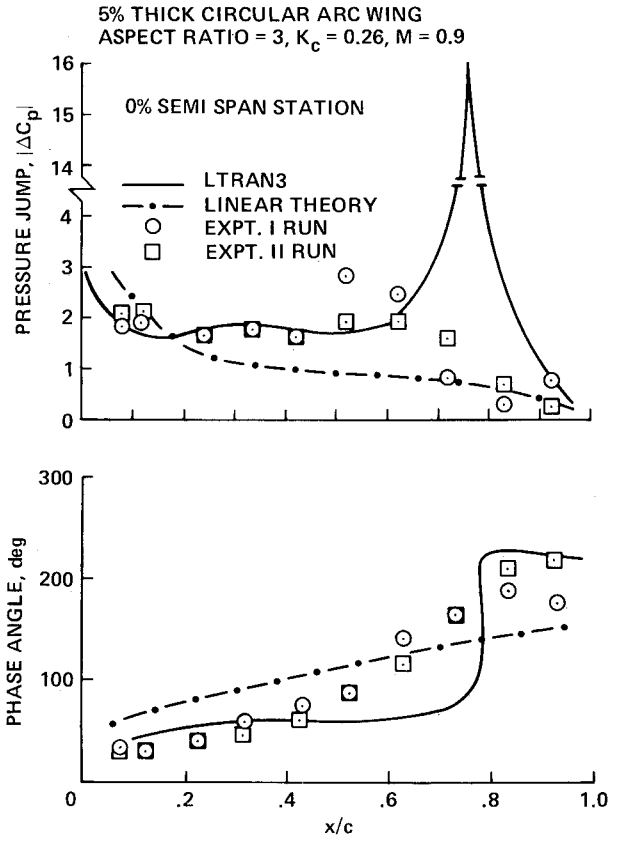

Fig. 3 Comparison of magnitude and corresponding phase angle of pressure jumps among results obtained by LTRAN3, experiment, and linear theory at root.

the unsteady pressure jumps and corresponding force coefficients were computed using the third cycle.

Aeroelastic Equations of Motion

The concept of generalized coordinates[20] is used in deriving the aeroelastic equations of motion. In this analysis two generalized coordinates, $h(t,y)$ and $\alpha(t,y)$, which correspond to bending displacement and torsional rotation of the elastic axis of the wing, were chosen as representative of the fluttering wing. The generalized coordinates $h(t,y)$ and $\alpha(t,y)$ can be expressed as

$$h(y,t) = \bar{h}(t)f(y); \qquad \alpha(y,t) = \bar{\alpha}(t)\theta(y) \tag{2}$$

where $\bar{h}(t)$ and $\bar{\alpha}(t)$ are unknown functions of time, and $f(y)$ and $\theta(y)$ are assumed semirigid modes.

The following sets of functions for $f(y)$ and $\theta(y)$, suggested by Fung,[20] were considered in this analysis:

$$f(y) = (y/l)^2; \qquad \theta(y) = y/l \tag{3}$$

The aeroelastic parameters and sign conventions for a typical section of the wing are shown in Fig. 1. It is assumed that the wing is rigid in the chordwise direction and the amplitudes of oscillation are small. It is also assumed that the principle of superposition of airloads is valid, even in the presence of shocks. The validity of this assumption has been shown for two-dimensional cases both by experiment[21] and theory,[16] provided the shock wave does not introduce separation.

Considering the inertia, elastic, and aerodynamic forces in generalized coordinates, the equations of motion are

$$\bar{m}\ddot{\bar{h}} + \bar{S}_\alpha \ddot{\bar{\alpha}} + \bar{m}\omega_h^2 \bar{h} = Q_h$$

$$\bar{S}_\alpha \ddot{\bar{h}} + \bar{I}_\alpha \ddot{\bar{\alpha}} + \bar{I}_\alpha \omega_\alpha^2 \bar{\alpha} = Q_\alpha \tag{4}$$

where

$$\bar{m}=\int_0^{\ell} m(y)f^2(y)\,dy \quad \text{generalized mass}$$

$$\bar{I}_\alpha=\int_0^{\ell} I_\alpha(y)\theta^2(y)\,dy \quad \text{generalized mass moment of inertia}$$

$$\bar{S}_\alpha=\int_0^{\ell} S_\alpha(y)f(y)\theta(y)\,dy \quad \text{generalized static moment}$$

and $m(y)$, $S_\alpha(y)$, and $I_\alpha(y)$ denote distribution of mass, static moment, and mass moment of inertia along the wing, respectively; ω_h and ω_α represent frequencies corresponding to the first bending mode h and first torsional mode α, respectively; and Q_h and Q_α are generalized aerodynamic forces corresponding to the modes $f(y)$ and $\theta(y)$, respectively.

After nondimensionalizing and assuming harmonic oscillations

$$\bar{\xi}=\xi_0 e^{i\omega t}; \qquad \bar{\alpha}=\alpha_0 e^{i\omega t} \tag{5}$$

with flutter frequency ω, Eq. (1) can be written as

$$\begin{aligned} -\xi_0-\bar{x}_\alpha\alpha_0+\xi_0(\omega_h/\omega)^2 &= Q_h e^{-i\omega t}/2\pi\bar{\mu}\ell bqk_b^2 \\ -\bar{x}_\alpha\xi_0-\bar{r}_\alpha^2\alpha_0+\bar{r}_\alpha^2(\omega_\alpha/\omega)^2\alpha_0 &= Q_\alpha e^{-i\omega t}/2\pi\bar{\mu}\ell b^2 qk_b^2 \end{aligned} \tag{6}$$

where $\bar{\mu}=\bar{m}/\pi\rho\ell b^2$, $\bar{x}_\alpha=\bar{S}_\alpha/\bar{m}b$, $\bar{r}_\alpha^2=\bar{I}_\alpha/\bar{m}b^2$, and $\bar{\xi}=\bar{h}/b$.

Structural damping can be introduced into Eqs. (4) by replacing ω_h and ω_α by $\omega_h(1+ig_h)$ and $\omega_\alpha(1+ig_\alpha)$, respectively. The damping coefficients g_h and g_α correspond to the h and α modes, respectively. It is further assumed that g_h and g_α are small and of the same order.

If the aerodynamic forces Q_h and Q_α are expressed in terms of aerodynamic coefficients $\bar{C}_{\ell h}$, $\bar{C}_{\ell\alpha}$, $\bar{C}_{mh}$, and $\bar{C}_{m\alpha}$, Eqs. (4) yield the eigenvalue equations

$$\bar{\mu}k_b^2\left([M]-[A]\right)\begin{Bmatrix}\xi_0\\ \alpha_0\end{Bmatrix}=\lambda[K]\begin{Bmatrix}\xi_0\\ \alpha_0\end{Bmatrix} \tag{7}$$

where $k_b=\omega b/U$ is the reduced frequency. The matrices $[M]$, $[A]$, and $[K]$ are defined as follows:

$$[M]=\begin{bmatrix} 1 & \bar{x}_\alpha \\ \bar{x}_\alpha & \bar{r}_\alpha^2 \end{bmatrix} \tag{8a}$$

$$[A]=\frac{1}{\pi}\begin{bmatrix} \bar{C}_{\ell h}/2 & \bar{C}_{\ell\alpha} \\ -\bar{C}_{mh} & -2\bar{C}_{m\alpha} \end{bmatrix} \tag{8b}$$

$$[K]=\begin{bmatrix} (\omega_h/\omega_r)^2 & 0 \\ 0 & \bar{r}_\alpha^2(\omega_\alpha/\omega_r)^2 \end{bmatrix} \tag{8c}$$

where

$$\bar{C}_{\ell h}=\int_0^{\ell} C_{\ell h}f(y)^2\,dy$$

$$\bar{C}_{\ell\alpha}=\int_0^{\ell} C_{\ell\alpha}f(y)\theta(y)\,dy$$

$$C_{mh}=\int_0^{\ell} C_{mh}f(y)\theta(y)\,dy$$

$$C_{m\alpha}=\int_0^{\ell} C_{m\alpha}\theta(y)^2\,dy$$

and ω_r is a reference frequency.

The eigenvalue λ is defined as

$$\lambda=\bar{\mu}(1+ig)\omega_r^2 b^2/U^2 \tag{9}$$

where $g(=g_h=g_\alpha)$ is the structural damping coefficient which is assumed to be small and of the same order for both of the assumed modes. The flutter solution is obtained when the g value corresponds to the average of the two modes.

Flutter Solution Procedure

In Ref. 4, a procedure based on the U-g method was successfully employed to determine the transonic flutter boundaries of airfoils. In the present work, the same procedure is extended to predict the flutter boundaries of wings.

Unsteady aerodynamic coefficients required in this work were the generalized lift and moment coefficients owing to modal motions corresponding to a pure bending mode $f(y)$ and a pure torsional mode $\theta(y)$. From the studies made using NASTRAN it was found that these two modes were sufficient to compute flutter boundaries within reasonable accuracy.

To solve Eqs. (7) by the U-g method, unsteady aerodynamic coefficients $\bar{C}_{\ell h}$, $\bar{C}_{\ell\alpha}$, $\bar{C}_{mh}$, and $\bar{C}_{m\alpha}$ are required as a function of reduced frequency for each mode. In this analysis the coefficients were computed at three reduced frequencies and they were interpolated by a Lagrange interpolation scheme. Since a low-frequency assumption was used in LTRAN3, the reduced frequencies considered were less than 0.4 (based on full chord).

Results

Comparison of Aerodynamic Pressure Coefficients

In Ref. 11, experimental investigations were conducted on an unswept rectangular wing in the 6×6-ft supersonic wind tunnel at Ames Research Center; the tunnel is a closed-return, variable-pressure facility capable of furnishing a continuous Mach number range from 0.70 to 2.20. The wings had an aspect ratio of 3 with a 5% thick biconvex airfoil section. The model was 27.44 in. in the span direction and 18.0 in. in the chord direction. Both steady and unsteady pressures were measured. Unsteady pressures were measured while the wing was oscillating in its first bending mode with a tip amplitude of 0.2 in.

Table 1 Comparisons of flutter speed and corresponding reduced frequency between LTRAN3 and experiment

Case	Mach No.	Thickness ratio, %	Density ratio, $m/\pi\rho b^2$	Reduced frequency, $\omega c/U$		Flutter speed, $U/b\omega_\alpha$	
				LTRAN3	Expt.	LTRAN3	Expt.
1	0.715	6	36.72	0.250	0.232	4.30	3.83
2	0.851	6	58.72	0.120	0.162	5.60	4.55
3	0.913	6	74.65	0.045	0.122	8.80	4.94
4	0.904	4	75.17	0.085	0.138	6.60	3.70

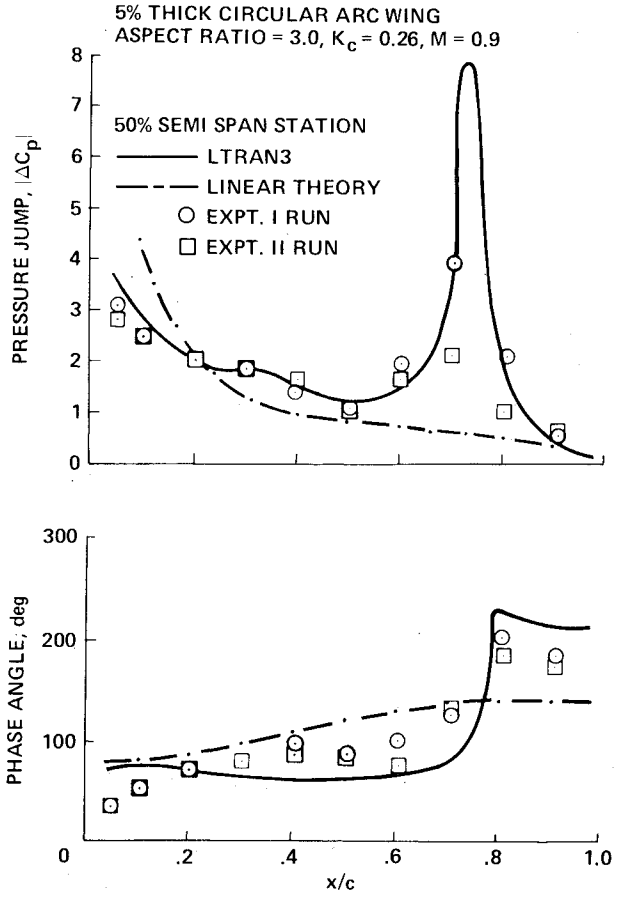

Fig. 4 Comparison of magnitude and corresponding phase angle of pressure jumps among results obtained by LTRAN3, experiment, and linear theory at 50 percent semispan.

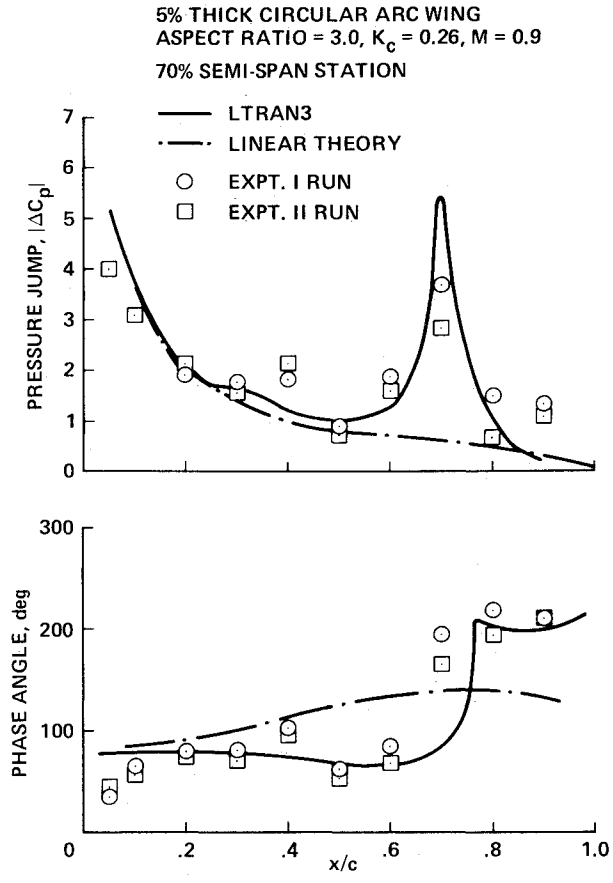

Fig. 5 Comparison of magnitude and corresponding phase angle of pressure jumps among results obtained by LTRAN3, experiment, and linear theory at 70 percent semispan.

In this study, steady and unsteady pressures from LTRAN3 are compared with experimental data[11] at Mach numbers of 0.7 and 0.9 for four span stations located at 0, 50, 70, and 90% semispan. For unsteady computations the same bending mode that was measured in the experiment was also simulated in the code. These results are also compared with corresponding data obtained in Ref. 11 in which linear aerodynamic theory, based on the kernel function method, was used. In the following results, the magnitude of the unsteady pressure jump is scaled by the induced angle of attack corresponding to the amplitude of the tip displacement, and the phase angle is defined as positive if the pressure leads the bending displacement. The magnitude and phase angle from LTRAN3 correspond to the first fundamental harmonic in a Fourier series decomposition of the pressure time history.

Comparison between LTRAN3 and experiment of both steady and unsteady results are adequate at $M = 0.70$.[22] In this paper, results at $M = 0.9$ are given.

In Fig. 2, steady-pressure curves are compared between experiment and LTRAN3 at $M = 0.9$ at four spanwise stations. The two sets of curves compare fairly well. Except at the root section, pressure coefficients and shock locations obtained by LTRAN3 are in close agreement with those obtained from the experiment. The discrepancies at the root section can be attributed mainly to the boundary layer on the wall, which was not considered in LTRAN3.

In Figs. 3-6, magnitudes $|\Delta C_p|$ and phase angles Φ of the unsteady pressure jump obtained by LTRAN3, experiment, and kernel function method are plotted at 0, 50, 70, and 90% semispan stations, respectively, for $M = 0.9$ and $k_c = 0.26$. In general, the two sets of curves obtained by LTRAN3 and experiment compare fairly well, except near the root. The magnitude of the pressure coefficients compare better than

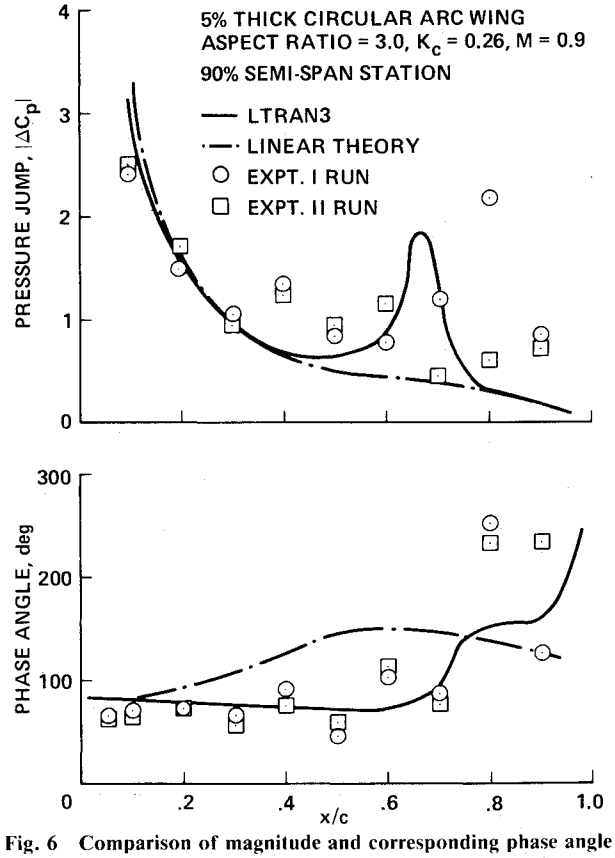

Fig. 6 Comparison of magnitude and corresponding phase angle of pressure jumps among results obtained by LTRAN3, experiment, and linear theory at 90 percent semispan.

phase angles. Peaks in pressure jumps occur at almost the same locations for both LTRAN3 and experiment. The comparison of phase angles is more favorable for points away from the shock. Linear theory results do not compare favorably, either with LTRAN3 or experiment, in the vicinity of the shock, as expected.

In Figs. 2-6, discrepancies between LTRAN3 and experimental results might be attributed to 1) the viscous effects, which are not considered in LTRAN3; 2) the reflection in the flow boundaries in the code,[23] 3) the wind tunnel wall effects; or 4) the fact that the small-disturbance theory has a tendency to overpredict the shock strength.

Comparison of Flutter Boundaries

Reference 13 reports an experimental investigation that was conducted in the Langley 2-ft transonic aeroelasticity tunnel to study the transonic flutter characteristics of unswept rectangular wings of aspect ratio 5 with circular-arc sections at various thickness ratios and Mach numbers. The model was 11.50 in. in the spanwise direction and in the 4.56 in. chordwise direction. The elastic axis and the center of gravity were located at the midchord. Thus, x_α and a_h were zeros for all wing sections. The first bending frequency, ω_h, was 89.2 rad/s, and the first torsional frequency, ω_α, was 505.2 rad/s for the 6% thick wing. The corresponding frequencies for the 4% thick wing were $\omega_h = 87.3$ rad/s and $\omega_\alpha = 507.7$ rad/s.

In this study, results obtained from LTRAN3 and from experiments are compared for four cases: 1) 6% thick at $M=0.715$, 2) 6% thick at $M=0.851$, 3) 6% thick at $M=0.913$, and 4) 4% thick at $M=0.904$. These cases were selected so that Mach numbers from a no-shock case to a strong-shock case were included. Based on studies using LTRAN3, the Mach numbers considered in the experiment did not include a moderate-shock case for the 6% thick model. Thus, a case from the 4% thick model was selected.

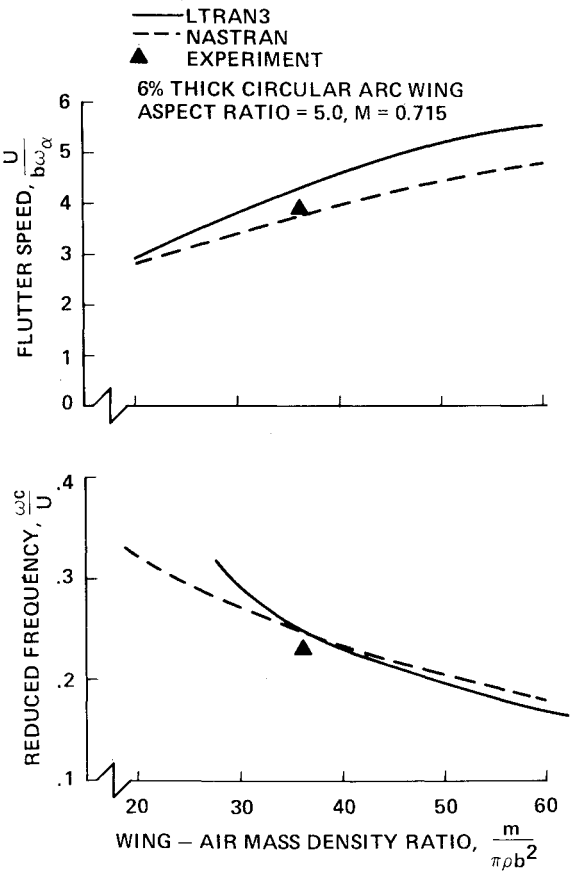

Fig. 7 Comparison of flutter speed and corresponding reduced frequency among results obtained by LTRAN3, experiment, and NASTRAN for case 1.

To understand the nature of the flow, steady-state pressures were computed for all of the cases.[22] It was observed that for the 6% thick model at $M=0.715$, the flow is subsonic completely; at $M=0.851$, the flow started becoming supersonic. At $M=0.913$, shocks are fairly strong. For a 4% thick model, shocks are moderate for $M=0.904$.

Unsteady aerodynamic coefficients were obtained for two assumed modes at three reduced frequencies.[22] Frequencies were selected based on those given in the experiment. For case 1 the reduced frequencies considered were 0.2, 0.232, and 0.3. For all other cases, the reduced frequencies selected were 0.1, 0.15, and 0.2. The generalized unsteady aerodynamic coefficients $\bar{C}_{\ell h}$, $\bar{C}_{\ell\alpha}$, $\bar{C}_{mh}$, and $\bar{C}_{m\alpha}$ were obtained based on the time response of the lifts and moments for a forced sinusoidal motion. For all four cases considered, an amplitude equivalent to 0.01 rad of induced angle was used. It was observed that all cases required about three cycles to give periodic responses.

Based on the unsteady aerodynamic coefficients obtained from LTRAN3, flutter boundaries were computed by the *U-g* method. In Fig. 7, results from LTRAN3 are plotted as a curve of flutter speed and corresponding reduced frequency vs wing-air-mass-density ratio for 6% thick model at $M=0.715$. The corresponding curve obtained by NASTRAN is given in the same figure. The experimental results available for a wing-air-mass-density ratio of 36.72 and a reduced frequency of 0.232 are also shown.

In Fig. 7, flutter results obtained by LTRAN3 and NASTRAN compare fairly well. The flutter speed obtained by experiment lies between those obtained by LTRAN3 and NASTRAN. The reduced frequencies obtained from the experiment are slightly lower than those obtained by theoretical methods. From this it may be concluded that the three methods compare well at the subsonic Mach number of 0.715. Also, the two modes assumed in Eqs. (3) are sufficient to represent the cantilever wings considered.

Similar results were obtained for the other three cases. Results for the four cases are given in Table 1. From this table it can be observed that the flutter speeds obtained by LTRAN3 are greater than those obtained by experiment. On the other hand, the reduced frequencies obtained by LTRAN3 are lower than those obtained by the experiment, except for case 1. With the increase in Mach number, both LTRAN3 and the experiment show an increase in flutter speed, a decrease in reduced frequency, and an increase in density ratio. Comparisons are better at lower Mach numbers. Differences are quite significant at $M=0.904$ and 0.913. These differences can be attributed mainly to the possible discrepancies between the aerodynamics of LTRAN3 and the experiment rather than flutter modeling.

Conclusions

In this study some comparisons are made between the results obtained by a three-dimensional unsteady code LTRAN3 and available experimental data from NASA. Based on aerodynamic comparisons it can be concluded that LTRAN3 compares fairly well at Mach numbers of 0.7 and 0.9. Discrepancies found at $M=0.9$ may be due mainly to the fact that viscous effects are not considered in LTRAN3. Comparisons of flutter results show that LTRAN3 compares well with experiment at low transonic Mach numbers. However, significant differences were seen at high transonic Mach numbers such as 0.913. In general, the reasons for discrepancies between LTRAN3 and experiment can be attributed to: 1) viscous effects not considered in LTRAN3; 2) limitations of small-disturbance theory, such as its tendency to overpredict shock strengths; 3) reflections of the flow boundaries in the code; and 4) wind tunnel wall effects and model scale effects in experiment.

Acknowledgments

The authors would like to thank Drs. Carson Yates and Robert Bennett of NASA Langley Research Center for their valuable suggestions during this research. The authors are also thankful to Mr. Chris Borland of Boeing in Seattle, Washington, and Mr. Malden Chargin of NASA Ames Research Center, for consultation in the use of LTRAN3 and NASTRAN, respectively.

References

[1] Ballhaus, W.F. , Deiwert, G.S., Goorjian, P.M., Holst, T.L., and Kutler, P., "Advances and Opportunities in Transonic Flow Computations," *Numerical and Physical Aspects of Aerodynamic Flows*, Springer-Verlag, New York, N.Y., 1982, pp. 371-396.

[2] Ashley, H., "Role of Shocks in the 'Sub-Transonic' Flutter Phenomenon," *Journal of Aircraft*, Vol. 17, March 1980, pp. 187-197.

[3] Ballhaus, W.F. and Goorjian, P.M., "Implicit Finite Difference Computations of Unsteady Transonic Flows About Airfoils," *AIAA Journal*, Vol. 15, Dec. 1977, pp. 1728-1735.

[4] Yang, T.Y., Guruswamy, P., Striz, A.G., and Olsen, J.J., "Flutter Analysis of a NACA 64A006 Airfoil in Small Disturbance Transonic Flow," *Journal of Aircraft*, Vol. 17, April 1980, pp. 225-232.

[5] Rizzetta, D.P., "The Aeroelastic Analysis of a Two Dimensional Airfoil," *AIAA Journal*, Vol. 16, Jan. 1979, pp. 117-124.

[6] Traci, R.M., Albano, E.D., and Farr, J.L., "Small Disturbance Transonic Flows About Oscillating Airfoils and Planar Wings," AFFDL-TR-75-100, June 1975.

[7] Eastep, F.E. and Olsen, J.J., "Transonic Flutter Analysis of a Rectangular Wing with Conventional Airfoil Sections," *AIAA Journal*, Vol. 18, Oct. 1980, pp. 1159-1164.

[8] Borland, C.J., Rizzetta, D.P., and Yoshihara, H., "Numerical Solution of Three Dimensional Unsteady Transonic Flow Over Swept Wings," AIAA Paper 80-1369, Snowmass, Colo., July 1980.

[9] Borland, C.J. and Rizzetta, D.P., "Nonlinear Transonic Flutter Analysis," AIAA Paper 81-0608-CP, AIAA Dynamic Specialist Conference, Atlanta, Ga., April 1981.

[10] Davis, S.S. and Malcolm, G.M., "Transonic-Shock Wave/Boundary Layer Interaction on an Oscillating Airfoil," *AIAA Journal*, Vol. 18, Nov. 1980, pp. 1306-1312.

[11] Lessing, H.C., Troutman, J.L., and Menees, G.P., "Experimental Determination of the Pressure Distribution on a Rectangular Wing Oscillating in First Bending Mode for Mach Numbers from 0.24 to 1.30," NASA TN D-344, 1960.

[12] Tijdeman, H. et al., "Transonic Wind Tunnel Tests on an Oscillating Wing with External Stores; Part I—General Description," AFFDL-TR-78-194, Part I, Dec. 1978.

[13] Doggett, R.V., Rainey, A.G., and Morgan, H.G., "An Experimental Investigation of Aerodynamic Effects of Airfoil Thickness on Transonic Flutter Characteristics," NASA TM X-79, 1959.

[14] Farmer, M.B. and Hanson, P.W., "Comparison of Supercritical and Conventional Wing Flutter Characteristics," NASA TM X-72837, 1976.

[15] Ballhaus, W.F. and Goorjian, P.M., "Computation of Unsteady Transonic Flows by the Indicial Method," *AIAA Journal*, Vol. 16, Feb. 1978, pp. 117-126.

[16] Guruswamy, P. and Yang, T.Y., "Aeroelastic Time Response Analysis of Thin Airfoils by Transonic Code LTRAN2," *Computers and Fluids*, Vol. 9, No. 4, Dec. 1980, pp. 409-425.

[17] Yoshihara, H., "Formulation of the Three-Dimensional Transonic Unsteady Aerodynamic Problem," AFFDL-TR-79-3030, Feb. 1979.

[18] Ballhaus, W.F., Bailey, F.R., and Frick, J., "Improved Computational Treatment of Transonic Flow About Swept Wings," *Advances in Engineering Sciences*, Vol. 4, Nov. 1976, pp. 1311-1320.

[19] Borland, C.J. and Rizzetta, D.P., "Transonic Unsteady Aerodynamics for Aeroelastic Applications. Vol. I: Technical Development Summary," AFFDL-TR-80-3107, Vol. I, June 1982.

[20] Fung, Y.C., *Theory of Aeroelasticity*, Dover Publications, Inc., New York, 1969.

[21] Davis, S. and Malcolm, G., "Experiments in Unsteady Transonic Flow," AIAA Paper 79-0769, April 1979.

[22] Guruswamy, P. and Goorjian, P.M., "Comparisons between Computations and Experimental Data in Unsteady Three-Dimensional Transonic Aerodynamics, Including Aeroelastic Applications," AIAA Paper 82-0690-CP, AIAA/ASME/ASCE/AHS 23rd Structures, Structural Dynamics and Materials Conference, May 1982, pp. 277-289.

[23] Kwak, D., "Non-Reflecting Far-Field Boundary-Conditions for Unsteady Transonic Flow Computation," AIAA Journal, Vol. 19, Nov. 1981, pp. 1401-1407.